BMC Microbiology

RESEARCH

Open Access

The natural symbiotic bacterium *Enterococcus faecalis* LX10 drives *Bombyx mori* refractoriness to *Nosema bombycis* infection *via* the secretion of enterococcin

Xiancui Zhang[1], Liang Yang[3], Tong Cai[5], Haoran Liao[1], Peiwen Cai[1], Xinkuang Zhao[1], Nengjie Gu[1], Zihan Yue[1], Yanzhou Gu[1], Fan Zhang[4], Choufei Wu[1*] and Xingmeng Lu[2*]

Abstract

Background The microsporidian *Nosema bombycis* is an obligate intracellular fungal-related parasites of the *Bombyx mori*, causing the epidemic disease Pebrine and extensive economic losses in the agricultural and sericulture industry. *Enterococcus* has emerged as one of the predominant gut microorganisms of the major model organism, *Bombyx mori*. However, the potential interactions mechanism between *B. mori*, *N. bombycis* and *Enterococcus* have not been well demonstrated.

Methods To address this gap, we used an insect model, silkworm to examine the potential mechanism of the natural symbiotic bacterium *Enterococcus faecalis* LX10 drives *B. mori* refractoriness to *N. bombycis* infection. *E. faecalis* LX10 was isolated from the gut of healthy silkworms, and its inhibitory activity against *N. bombycis* was evaluated at both the cellular and individual levels using posttranslational modifications, gene and protein expression analysis, transfected cells, and in vitro immunofluorescence.

Results We demonstrated that enterococcin (EntLX), the first antimicrobial protein family in gut commensal bacterium *Enterococcus faecalis* LX10 of *B. mori*, contributes to defending against *N. bombycis* infection resistance depends on the enzyme gelatinase (GelE), disulfide bond and disulfide bond formation proteinA (DsbA). The EntLX protein, abundantly expressed in transgenic BmN cells and gut organs(gut epithelium, peritrophic membrane and contents), can reduce the infection rate of cells and alleviate intestinal damage caused by *N. bombycis* infection. After simultaneous vaccination with *E. faecalis* LX10 and *N. bombycis*, the differentially key metabolites, physiological characteristics(larval mass), or economic traits(cocoon length, cocoon width, whole-cocoon weight, cocoon shell weight, pupation rate and adult emergence rate) showed a certain degrees of recovery and correction compared with those of single *N. bombycis* inoculation at the individual level.

*Correspondence:
Choufei Wu
02407@zjhu.edu.cn
Xingmeng Lu
xmlu@zju.edu.cn

Full list of author information is available at the end of the article

Conclusions This study advances the understanding of the anti-microsporidia activity of enterococci and paves the way for the expression of these molecules as antifungal agents *via* the genetic transformation of *Enterococcus* symbionts from disease-transmitting insects.

Clinical trial number Not applicable.

Keywords *Bombyx mori*, *Nosema bombycis*, *Enterococcus faecalis*, Enterococcin, Symbionts

Introduction

Microsporidians are a widely distributed group of fungal-related intracellular pathogens that can invade almost all invertebrates and vertebrates, as well as immunocompromised humans [1, 2]. Among the 200 genera of Microsporidians, 93 are important biological control agents for agricultural and forestry pests or economically significant insects [3]. Silkworm pebrine disease has been identified as caused by *N. bombycis*, the first microsporidial species to be described as the causal agent [4, 5]. Pebrine infection caused by microsporidian spores is currently the only disease that has a mandatory quarantine due to its destructive effects on silk production [6].

Microsporidians are mainly *Nosema* species, the spores of which are transmitted through the fecal-oral route at all development stages and vertically from adults to offspring [1]. For successful transmission, microsporidia must complete a complex developmental program in the silkworm midgut, where they penetrate the gut epithelium, absorb nutrients and export cytotoxic compounds into the newborn spore host environment *via* the cell membrane [4]. Most microsporidia inflict sublethal impacts on insects, leading to diminished foraging efficiency and escalated mortality in silkworms. Moreover, eradicating these infections poses a significant challenge [2, 7]. There are alternatives to removing pebrine outbreaks, including selecting tolerant silkworm strains, augmenting immunity, or treating *N. bombycis* [8–10]. In addition to creating a good breeding environment by using disinfectants [11, 12], Pasteur's method of selecting uninfected offspring remains the most effective means of preventing and controlling pebrine disease [13]. The therapeutic effect of physical processes and chemical drugs on microsporidia infection has been demonstrated for bees and silkworms. For example, heat therapy has proven to be effective at eliminating or reducing microsporidian infections in insects [14]. In vitro, albendazole proved effective against *N. bombycis* without causing negative effects to the silkworm [3, 15]. Although these methods are effective, whether physical or chemical, is indisputable, their application in production has not received sufficient recognition.

As the first site of interaction between pathogens and hosts, the gut and commensal microbiota play key roles in protecting the host from exogenous pathogen infections, making the gut compartment a prime candidate target for pebrine intervention [16–19]. Although exactly how commensal bacteria confer benefit to the host is unclear, probiotics may restore epithelial barrier function [20–22], improve microbial balance [23], compete with pathogens for adhesion sites [24] and boost epithelial immune responses [25, 26], thereby preventing infection and pathology. There are gram-positive and gram-negative bacteria inhabiting the silkworm gut [27]. Recent studies have revealed *Enterococcus*, *Lactococcus*, *Stenotrophomonas*, *Bacillus*, and *Pseudomonas* are the predominant gut bacteria [28]. Our previous study showed that higher abundances of *Enterococcus*, *Escherichia-Shigella*, *Staphylococcus*, and *Glutamicibacter* after infection, while only *Enterococcus* had a strong correlation with inoculation time and infection concentration by 16 S rRNA gene sequence analysis [29]. Therefore, the dominant species, *E. faecalis*, is particularly likely to play a major role in facilitating the survival of its host in a changing environment during development. In addition, the intestinal commensal bacterium *Enterococcus* reduced the infection rate of *N. bombycis*, suggesting that *E. faecalis* produces enterococcin, which may affect *N. bombycis* in part [29]. Although *E. faecalis* LX0 protection has been demonstrated in principle, there is still a gap in understanding of its molecular basis and functionality.

To address this principal objective, the interaction mechanism of silkworm-*N. bombycis*-*E. faecalis* LX0 was investigated. First, we studied the posttranslational processing modifications required for the anti-*N. bombycis* activity of enterococcin (EntLX), which is secreted from *E. faecalis* in the gut. Additionally, to further evaluate this anti-*N. bombycis* activity mechanism, we performed gene and protein expression analysis, constructed engineered strains, transfected cells, and performed immunofluorescence in vitro and at the cellular and individual levels. Finally, we analyzed critical economic traits and metabolic functions after simultaneous inoculation of *E. faecalis* LX10 and *N. bombycis.*

Materials and methods

Silkworms, cell lines, bacterial strains, and *N. bombycis*

The hybrid *B. mori* strain Haoyue×Jingsong was obtained from the Silkworm Germplasm Bank of the Cathaya Group, Chun an, Zhejiang, China (118°71'N, 29°36'E). Germ-free larvae (GF) were prepared by surface

sterilizing silkworm eggs with sodium hypochlorite solution (1%, NaClO). Afterwards, the eggs were washed in sterile water after being immersed in ethanol (70%). GF conditions were validated by culturing fecal samples in Petri dishes. The insects were raised on an autoclaved artificial diet under standard conditions (25 °C, 70% humidity) [30].

The plasmids and strains used are listed in Supplementary Table 1. The ovarian cell line of *Bombyx mori* (BmN cells) were grown at 27 °C in Sf-900 II SFM (Invitrogen Life Technologies) supplemented with 10% fetal bovine serum (FBS; Gibco, US). The *N. bombycis* ZJU1 was obtained from the Institute of Sericulture and Apiculture, Zhejiang University.

Whole-genome sequencing

Genomic DNA from *E. faecalis* LX10 was obtained using a MasterPure™ Purification Kit (Epicenter, USA) [31]. The quality of DNA was determined a Qubit fluorometer (Thermo, Germany). Subsequently, the paired-end sequencing was performed at Majorbio Biopharm Technology Co., Ltd. (Shanghai, China) using an Illumina MiSeq platform. Low-quality reads and reads with ambiguous bases were filtered out by SMRT Analysis software version 2.3.0 [32]. The raw dataset, with an average length of 14,796 bp. Glimmer V3.02 software was utilized for gene prediction of strain LX10.

Recombinant expression, proteolytic cleavage of EntLX and anti-*N. bombycis* activity

The coding region of the EntLX136 (residues 35–171) gene was ligated into the pET-28a vector (Merck, Germany) between the cutting sites BamHI (GGATCC) and XhoI (CTCGAG) using T4 DNA Ligase (Vazyme, Nanjing, China). pET-28a-EntLX136 was transformed into *E. coli* BL21 (DE3) cells (Vazyme, Nanjing, China). Strain DE3 was cultured in LB media, induced to express with 1 mM IPTG. The bacterial cells were disrupted by using a Bacterial Protein Extraction Kit from Sangon Biotech (Shanghai, China). The supernatant was subsequently separated via 15% SDS–PAGE. The EntLX136 proteins were purified by Ni-NTA agarose (QIAGEN, Germany).

The *E. faecalis* system regulator (Fsr) is the major quorum-sensing (QS) system in *E. faecalis*. However, the Fsr system, which regulates gelatinase (GelE), was implied to be involved *via* genetic approaches [33, 34], but whether GelE directly acts on EntLX has not been determined. To further confirm that GelE directly proteolytic cleavage cleaves EntLX and contributes to the inhibition of *N. bombycis* germination activity, we examined EntLX processing using purified proteins [35]. Briefly, the GelE protein of *E. faecalis* LX10 was commissioned by HUABIO, Hangzhou, China. The *E. faecalis* LX10 used for GelE production. The culture medium of *E. faecalis* LX10 with an OD_{600} of 0.05 was centrifuged and filtered with 0.22-μm filters. Ammonium sulfate crystal was added to achieve at 4 °C, and the mixture was allowed to stand overnight. The slurry was centrifuged, the supernatant discarded, and the pellet resuspended in 50 mM Tris-HCl–1 mM CaCl2 (pH = 7.8). The dialyzed sample was concentrated using a stirred-cell concentrator (10,000 MWCO, Millipore, USA). The concentrate was applied at 1 ml/min to a preconditioned HiPrep 16/60 Sephacryl S-200 column (GE Healthcare). Then, EntLX136 (30 μg/ml) and GelE (1.25, 2.5, 5, 10, 15 and 20 μg/ml) were incubated for 1 h in PBS. The samples were boiled in sample buffer with mercaptoethanol at 100 °C to terminate the reaction. Purified EntLX136 was incubated similarly to the controls. Following 15% SDS-PAGE gel electrophoresis (Thermo Fisher Scientific, MA, USA), samples were stained with Coomassie Brilliant Blue (Biyuntian, China) to evaluate cleavage of rEntLX136.

Initial attempts to express and purify EntLX68 (residues 103–171) were unsuccessful in *E. coli*, perhaps due to its toxicity. Using an alternative method, the disulfide bond of the peptide with (EntLX68+) or without the disulfide bond (EntLX68-) was synthesized by standard solid-phase peptide synthesis (SPPS) protocols. Chem Impex Tentagel S-Ram 0.2–0.8 meq/g beads were used to synthesize the peptides starting from the C-terminus. Hydroxybenzotriazole (HOBt), N,N-diisopropylethylamine (DIPEA), and hexafluorophosphate benzotriazole tetramethyl uranium (HBTU) were used to catalyze the reactions. After the final deprotection, the beads were washed with dichloromethane (DCM). The dots were acid cleaved with Reagent B (5% phenol, 88% v/v trifluoroacetic acid, 2% triisopropylsilane, 5% ddH_2O). Before analysis, prior ether precipitation, DMSO dissolution, and lyophilization were performed on the peptides.

To evaluate the anti-*N. bombycis* activity of EntLX136, EntLX68+, and EntLX68-, *N. bombycis* suspension (20 μL, 10^7 spores/mL) was added to 96-well microplates containing 30 μL of enterococcin protein (EntLX136, EntLX68+, and EntLX68-) at different concentrations (0.002, 0.02, 0.2, 2 mg/mL). An equal amount of phosphate buffer (pH = 6) was used as a control (CK). GKK germination buffer (0.05 M KOH, 0.05 M glycine, and 0.375 M KCl; pH = 10.5) was then added, and the samples were incubated at 27 °C for 60 min. The absorbance at 625 nm (OD625) was measured using a microplate reader both before(germination liquid initiation OD_{625}) and after(germination liquid termination OD_{625}) incubation to assess the germination rate. The following formula was used: germination rate = [(germination liquid initiation OD_{625}–germination liquid termination OD_{625})/germination liquid initiation OD_{625}] × 100%.

Reduction and alkylation of the supernatant

The fermentation broth supernatant was collected from culture at 37 °C during the logarithmic growth phase in MRS Broth (Hopebio, Qingdao, China). Subsequently, β-mercaptoethanol (0.2%, Sigma Aldrich, USA) was added to 500 mL of the supernatant, which was subsequently incubated at 26 °C for 1 h. The solution was supplemented with 0.2% 4-vinylpyridine (Sigma, USA). Afterward, an extra 2 h of incubation was carried out. Amicon Ultra 3 kDa (Millipore, MA, USA) was used for ultrafiltration to concentrate the medium at 4,000 g for 20 min. Using ice-cold HEPES buffer (5mM, Merch, Germany), the remaining concentrate was washed and then resuspended in HEPES. The reduced and alkylated media were readjusted to pH 6.0, after which the anti-*N. bombycis* activity was tested.

Construction of engineering strains and functional verification

To express EntLX in the isogenic EntLX-deficient strain (EntLX-, *E. faecalis* LX11, *E. mundtii*, and *E. casseliflavus*), EntLX gene fragments containing promoters and terminator were generated by gene synthesis between the BamHI and SalI restriction sites of the *Enterococcus* expression vector PAM401(ATCC 37429, Manassas, VA, USA) (Supplementary Table 3). Based on whole-genome sequencing data, the promoter sequence and the Rho-dependent terminator of the EntLX gene were predicted and analyzed using PromPredict software and TransTermHP software, respectively. Gene synthesis and sequencing were performed by Qingke Biotechnology (Qingke, Beijing, China). The recombinant vector (PAM401-EntLX) was electrotransformed into the *E. faecalis* LX11, *E. mundtii*, and *E. casseliflavus* strains using an Eppendorf Electroporator 2510 (Eppendorf, Hamburg, Germany) electroporator. This engineered strain was named EF, EM, and EC with chloramphenicol (Cm; 5 μg/ml) resistance for screening.

The PAM401 plasmid used to express the insertional mutants (Δ1-Δ7) was constructed similarly to the previously described plasmid PAM401 using *E. faecalis* LX11 as a template. The construction of insertion mutants is based on the positioning of the signal peptide and the two cysteine sites that form disulfide bonds. Briefly, the DNA deletion product (Δ1: delete 157–408 bp, includes partial signal peptide and first cystine at the disulfide bond formation site; Δ2: delete signal peptide 4–309 bp bp; Δ3: delete 216–408 bp, includes first cystine at the disulfide bond formation site; Δ4: delete 409–501 bp, including the second cystine at the disulfide bond formation site, Δ5: delete 316–318 bp, the first cysteine; Δ6: delete 499–501 bp, the second cysteine; Δ7: delete 376–441 bp, a small fragment between two cysteines) were cloned and inserted into PAM401 vector, respectively. The recombinant plasmid (PAM401-ΔEntLX) was extracted and further transformed into *E. faecalis* LX11. We further utilized engineered strains and insertional mutants with definite resistance mechanisms to test the anti-*N. bombycis* activity of these strains.

Polyclonal antibody preparation, cell transfection and immunofluorescence (IF)

The EntLX protein was prepared according to the method described above. New Zealand white rabbits were initial immunized with EntLX(1 mg/ml) protein with complete and incomplete Freund's adjuvant, respectively. The second immunization occurs 14 days after the first, with a 7-day interval between the second and third. Rabbit blood samples were collected, indirect ELISA was used to determine antiserum titers, and antibodies were purified. A 256,000-titer antibody was successfully prepared based on indirect ELISA results.

Enterococcin full-length DNA (Fig. 1) was PCR amplified from *E. faecalis* LX10 using the primers bac F/R and subcloned and inserted into the vector pIZ/V5-His with flag labels at the BamH-I and HindIII sites. The recombinant vector was transformed into *E. coli* TOP10 cells (Invitrogen, USA). According to the transfection protocol, plasmid DNA was extracted and introduced into the BmN cells (1×10^6) with Cellfectin™ II Reagent (Thermo, USA). After fixing with 4% paraformaldehyde for 20 min at 24, 48, and 72 h, the samples were permeabilized and subsequently incubated with anti-EntLX antibodies. Following incubation with tetramethyl rhodamine isothiocyanate(TRITC) goat anti-rabbit antibody (Invitrogen), the cells were treated with 4',6-diamidino-2-phenylindole (DAPI, Beyotime) for 20 min and visualized through confocal scanning laser microscopy (CSLM) (ZEISS, Germany).

The infection rate of *N. bombycis* (10^7 spores/mL) was determined with an LSM780 confocal microscope (Zeiss) and stained with DAPI after 1, 2, or 3 d. Then, the cell pellet fractions were collected and quantified using qPCR to determine the *N. bombycis* spore burden. A fragment of the *N. bombycis* gene was amplified using the primers ssu1092F and ssu1227R. A standard curve was constructed by utilizing the DNA of *N. bombycis* (1×10^0 to 1×10^{10} copies/μL). Cq values were used to calculate gene copies of *N. bombycis* using the standard curve. PCR was performed with the following cycling parameters: 95 °C for 5 min, followed by 40 cycles of 95 °C for 10 s, 60 °C for 10 s and 72 °C for 10 s.

Distribution and histopathological analysis of *E. faecalis* LX10 or EntLX in the silkworm gut

The distribution of EntLX secreted by LX10 from the gut epithelium, peritrophic membrane, and gut contents was investigated by feeding fifth-instar GF silkworm

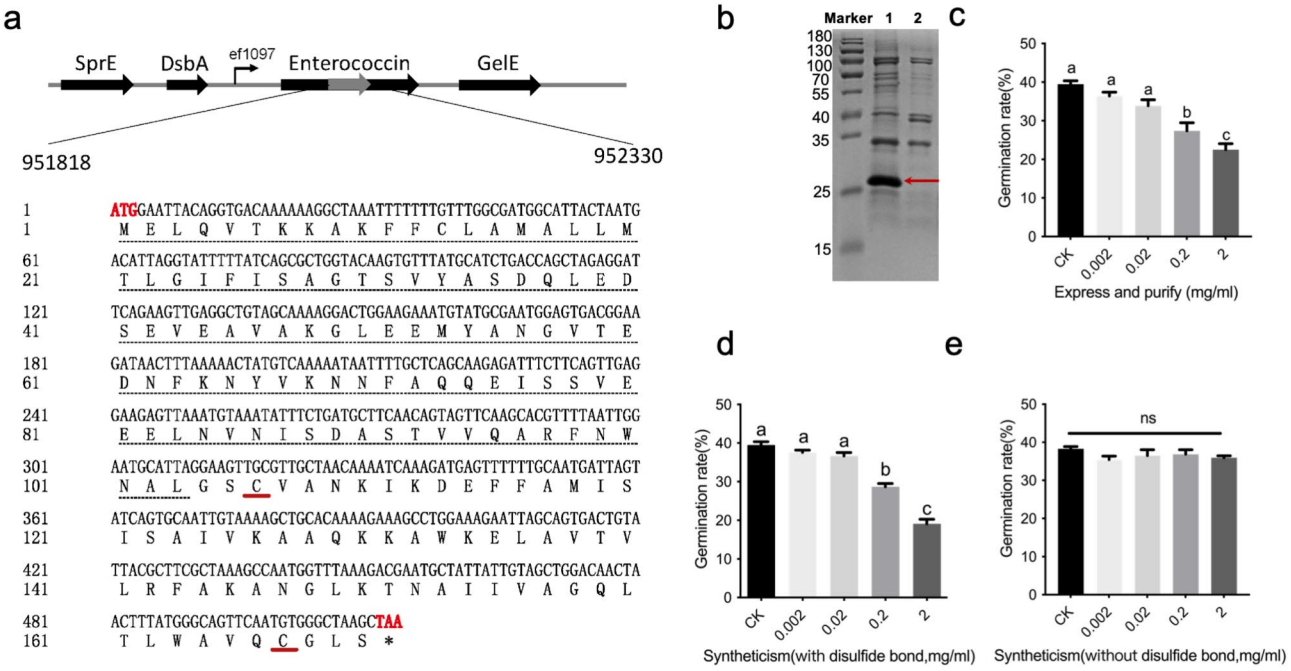

Fig. 1 Characterization of bacteriocin and inhibitory spectrum of *E. faecalis* LX10. **(a)** Genetic organization of the enterococcin (EntLX) protein corresponding to nucleotide sequences 951,818–952,330 and translation of the *E. faecalis* LX10 chromosome. The amino acid sequence of EntLX confirmed that the signal peptide (underlined) and the mature peptide consisted of 103 and 68 amino acids, respectively. The start and stop codons and cysteines used for disulfide bond generation are indicated in red. **(b)** Scheme for the overexpression of target proteins. Marker: 10–180 kDa, lane 1: EntLX of overexpressed recombinant strains detected by SDS-PAGE. The red arrows are bands of the target proteins. lane 2: extract of wild-type strain. Anti-*N. bombycis* assay of **(c)** EntLX136 and **(d)** EntLX68+ (a synthetic peptide containing a disulfide bond) in vitro at increasing concentrations (0.002, 0.02, 0.2, and 2 mg/mL) of EntLX68-(without the disulfide bond) **(e)**. The data were analyzed by using one-way ANOVA

larvae 25 μL of an LX10 cell suspension (1×10^7 CFU/mL), with healthy larvae as a negative control (CK). The expression levels of EntLX were determined by RT-qPCR analysis analysis at 0 d, 2, 4, and 6 d in fifth-instar GF silkworm larvae. Gut tissue (gut epithelium, gut contents, peritrophic membrane) was dissected on ice. The tissue samples were ground with two 5-mm zirconia beads at 5,000 rpm for 20 s using a Precells-24 homogenizer (Bertin Technologies, France). The CK and *E. faecalis* LX10 feeding groups were subjected to total RNA extraction using TRIZOL reagent (Thermo, USA). The manufacturer's instructions were followed (Vazyme Biotech Co., Ltd.) to reverse transcribe 1 μg of total RNA using HiScript® II RT SuperMix R223-01. The following primer (EntF/R) was used for RT−qPCR (Supplementary Table 2). The expression level of the housekeeping gene 16SrRNA was used as an endogenous control. The relative expression levels among the groups were calculated using the $2^{-\Delta\Delta}$ct method. RT-qPCR was performed according to a previously described method.

GF silkworm larvae of the fifth instar were divided into CK (50 μL sterile water), EntLX (25 μL EntLX + 25 μL sterile water), NB (25 μL *N. bombycis* + 25 μL sterile water), and NB + EntLX (25 μL EntLX + 25 μL *N. bombycis*) groups for the purpose of assessing the anti-*N. bombycis* activity of EntLX in vivo ($n = 15$) [29]. Each silkworm was inoculated with the same amount of EntLX (2 mg/mL) or *N. bombycis* suspension (1×10^9 spores/mL). Histopathological analysis of randomly selected gut samples was performed after 6 days. The gut was fixed in 4% polyformaldehyde fixing solution for fixing tissues, which were made into paraffin samples. The degree of gut pathological damage was assessed with periodic acid–Schiff (PAS) staining [36].

Untargeted metabolomics analysis

We divided the larvae of the fifth instar silkworm into four groups (CK, EF, NB, and NF). Each GF silkworm was fed an *E. faecalis* LX10 suspension (25 μL, 1×10^7 CFU/mL) or an *N. bombycis* suspension (25 μL, 1×10^9 spores/mL) (NF); an *E. faecalis* LX10 suspension (25 μL, 1×10^7 CFU/mL) and sterile water (25 μL, EF); or *N. bombycis* suspension (25 μL, 1×10^9 spores/mL) and the same amount of sterile water (NB). GF larvae were inoculated with 50ul sterile water as a control (CK). After 2, 4, and 6 days, guts ($n = 6$) were processed for untargeted metabolomics analysis. For each sample, gut epithelium tissues were collected and homogenized with liquid nitrogen to form a fine powder. The resuspension solution (100 μL, 0.1% formic) was added.

To ensure the quality of the metabolomic data, quality control samples (QC) were prepared using six replicate

samples (equal amounts). Metabolites were separated on an Agilent 1290 Infinity UHPLC, applying a gradient of ammonia in water (A) and 100% acetonitrile (B) from 5% A to 50% A for 12 min. The instrument was operated in negative and positive ion modes. The temperature of the column and autoinjector were kept at 25 °C and 5 °C, respectively. The source heater temperature for both modes was 550 °C. The METLIN database was used to identify the metabolites. Partial least squares discriminant analysis (PLS-DA) was performed by R packages. The metabolic differences between the CK treatment and treatment groups (EF, NB, and NF) were expressed as the average of positive (pos) and negative (neg) ions. Metabolite levels were subsequently calculated in MetaboAnalyst 3.0 based on the KEGG database (version 82.1), and topology analysis was performed using relative betweenness centrality.

Verification of the physiological function and economic traits of silkworms

The body masses of larvae from the treatment groups (EF, NB, and NF) and CK groups were weighed after 2, 4, and 6 d on an analytical balance. Pupation and adult emergence rates were calculated ($n = 60$). The mean whole cocoon weight, cocoon shell weight, cocoon length, and cocoon width were measured after cocooning using an electronic balance and a digital caliper ($n = 60$).

Statistical analysis

For the germination rate, the relative expression of EntLX, the absolute abundances of *N. bombycis*, larval mass, and economic traits and the metabolic differences were calculated *via* one-way analysis of variance (ANOVA) with Tukey's post hoc test or Student's t test. All experiments were repeated at least three times. Statistics were performed with Graphpad Prism 9.0 (Graphpad Prism, San Diego, CA, USA).

Results

Characterization of bacteriocin from *E. faecalis* LX10

E. faecalis LX10 is a strain isolated from the intestinal tract of silkworm. Complete genome sequencing revealed that the ef1097 gene is present in *the E. faecalis* LX10 strain sequenced and encodes a 171-aa prepeptide (EntLX); moreover, this gene belongs to a gene family that encodes antimicrobial proteins [37]. A nucleic acid sequence against the whole genome revealed that *E. faecalis* LX10 possesses the enterococcal protein (EntLX) (classified as a member of the antimicrobial protein family) biosynthesis gene, which matches that of the *E. faecalis* strain OG1RF based on BLAST searches (Fig. 1a). The complete nucleotide sequence of the EntLX protein was determined and found to total 513 bp (chromosome: 951818–952330) with a mol% G + C content of 36.26 mol%. The amino acid sequence of EntLX confirmed that the signal peptide and the mature peptide consisted of 103 and 68 amino acids, respectively, with molecular mass of 18.55 kDa. In addition, a predicted disulfide bond (amino acids 106–167) encompasses nearly the entire length of the active peptide (amino acids 103–171) (Fig. 1b).

Purification of the enterococcal protein and inhibition spectrum of *E. faecalis* LX10

Our previous studies in the *N. bombycis* infection model of *B. mori* revealed that the secreted inhibitor is a heat-stable peptide that tolerates a wide range of pH values [29]. To determine if EntLX alone is responsible for the inhibitory activity of *N. bombycis*, we isolated and purified EntLX136, which is an unprocessed peptide consisting of residues 35–171 aa. An evident band with a molecular weight of approximately 15.69 kDa was observed (Lane 1 in Fig. 1b, Fig S1). Inhibition of *E. faecalis* LX10 was investigated by a spore germination rate test. The purified EntLX136 protein showed significant inhibitory activity, and the inhibitory effect became more obvious ($F = 22.05$, $P < 0.0001$) with increasing EntLX136 concentration (Fig. 1c).

Due to its evident toxicity towards *E. coli*, the expression and purification of the mature peptide (68aa) were unsuccessful. Alternatively, the disulfide bond of the mature peptide with (EntLX68+) or without the disulfide bond (EntLX68-) was synthesized. EntLX68, which contains disulfide bonds, was more effective at inhibiting spore germination than was the unprocessed peptide, especially at high concentrations ($F = 91.83$, $P < 0.001$) (2 mg/mL). For example, EntLX68 + at 2 mg/mL reduced the germination rate of *N. bombycis* to less than 20% compared with that of the control group ($t = 9.656$, $df = 8$, $P < 0.001$) (Fig. 1d). The germination inhibition activity can reach up to 80%. However, it is important to note that the normal germination rate of *Nosema* spores in silkworms is approximately 40%. Therefore, the actual inhibition rate of 2 mg/mL EntLX68 in this study is around 50%. When disulfide bridges were absent, the mature peptide was almost completely inactivated ($F = 0.7826$, $P = 0.5511$) (Fig. 1e).

Moreover, three possible catalysts for disulfide bonds, thioredoxin, were identified within the *E. faecalis* genome called DsbA family protein (gene0494, chromosome: 505767–506285; gene0915, chromosome: 939624–940337; and gene2059, chromosome: 2188330–2188989). An X-ray crystallography consortium was used to determine the structure of thioredoxin, which has a site cysteines [38]. The gradual loss of anti-*N. bombycis* activity in enterococcal EntLX was observed upon disruption the cysteines site using 2-mercaptoethanol (Fig. 2a).

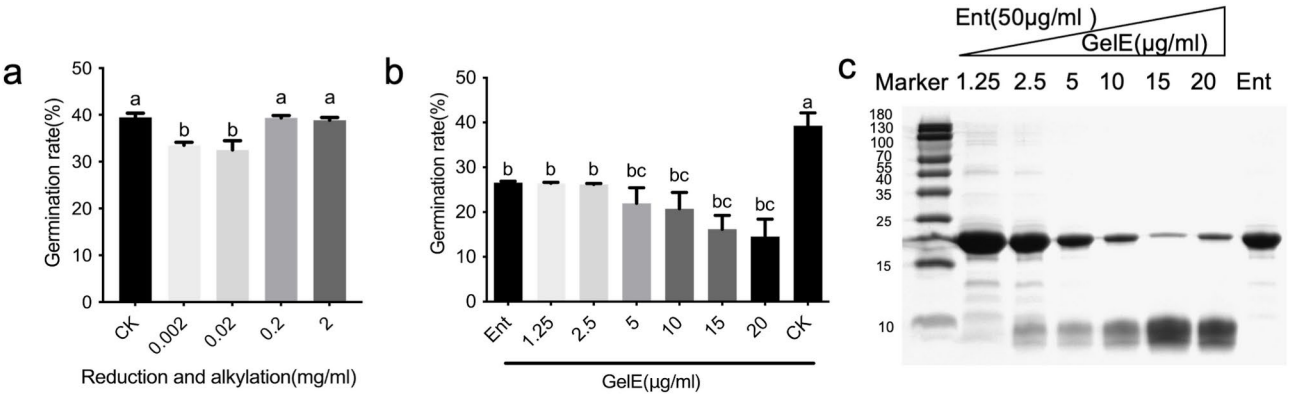

Fig. 2 Alkylation of EntLX and the cleavage process involving GelE and anti-*N. bombycis* activity. **(a)** Reduction and alkylation of the supernatant by 2-mercaptoethanol and 4-vinylpyridine reduce the activity against *N. bombycis*. **(b)** GelE is necessary for the inhibition of *N. bombycis* germination. EntLX136 (50 μg/ml) was incubated with GelE (1.25, 2.5, 5, 10, 15 and 20 μg/ml). **(c)** Cleavage process of EntLX by GelE based on SDS–PAGE

Gelatinase (GelE) was identified by genome sequencing, but whether GelE directly affects EntLX has not been determined. EntLX proteins were used to examine EntLX processing and anti-*N. bombycis* activity *in vitro.* GelE was purified from *E. faecalis* LX10, and then increasing concentrations of GelE were added to purified EntLX at 1.25–20 g/ml for 1 h. The higher the concentration of GelE applied was, the stronger its inhibitory effect on the germination rate of *N. bombycis* (Fig. 2b). Furthermore, full-length EntLX (15.69 kDa) was detected in the lanes lacking GelE. After the addition of GelE, EntLX was observed from a full-length (15.69 kDa) to a mature peptide (7.2 kDa) (Fig. 2c).

Efficient expression of enterococcal strains of engineered *Enterococcus* and the anti-*N. bombycis* effect in vitro

The constructed *E. faecalis* shuttle plasmid (PAM401) with the EntLX gene was transferred by electroporation into *E. faecalis* LX11, *E. mundtii*, and *E. casseliflavus* cells (without EntLX) named EF, EM and EC, respectively (Fig. 3a). A list of mutants of different lengths was subsequently constructed to determine the functional site of EntLX (Fig. 3b). Successful deletion of the different lengths of the EntLX gene and of the engineered strains were confirmed in all the selected colonies by both PCR and sequencing (Fig. 3bc). As expected, compared with the *Enterococcus* strains, the engineered strains with the EntLX genes of EF, EM, and EC strongly inhibited *N. bombycis* germination without the EntLX genes ($F = 21.07$, $P < 0.001$) (Fig. 3d). Further deletion of the disulfide bond fragment (△1, △3, △4, △5, △6) and signal peptide (△2) resulted in the complete loss of anti-*N. bombycis* activity ($F = 0.6072$, $P = 0.7209$) (Fig. 3d). However, deletion of the base sequence (66 bp) between the two disulfide bonds (106 aa and 167 aa) reduced only the activity of the anti-*N. bombycis* agent (△7) ($t = 4.213$, $df = 8$, $P = 0.0135$) (Fig. 3d). These data clearly show that disulfide bonding is essential for anti-*N. bombycis* activity.

Subcellular localization of EntLX and the anti-*N. bombycis* activity of BmN cells

Immunohistochemical assays revealed that transgenic EntLX proteins in BmN cells were localized in the cytoplasm at the early stage of transfection (24 h) and gradually diffused to the whole cytoplasm and nucleus with increasing transfection time (48–72 h) (Fig. 4a). We used an established EntLX transgenic cell model to quantitate the invasion of *N. bombycis. The results* showed a significant decrease in *N. bombyci* burden and infection rate was evident in transgenic cells relative to control silkworm treatment with *N. bombycis* (Fig. 4bc). For example, the number of intracellular gene copies in *N. bombycis* in normal cells and transgenic cells was 2.8×10^7 spores/sample and 1.3×10^7 pores/sample, respectively ($t = 5.635$, $df = 28$, $P < 0.0001$). These results further confirmed that the amount of *N. bombycis* that accumulated around the EntLX transgenic cells was significantly less than that around the normal cells (Supplementary Fig. S1).

Then, the EntLX gene expression levels of nucleus and cytoplasm in the same transgenic lines were determined by RT−qPCR (Fig. 4de). This confirmed that the EntLX was expressed mainly in the cytoplasm at the early stage of transfection (24–48 h) and in the nucleus at the late stage of transfection (72 h), consistent with previous results from immunohistochemical assays (Fig. 4de).

Expression of EntLX in the gut and its effect on *N. bombycis* in vivo

The mRNA and protein expression levels of EntLX in silkworm intestinal tissues were subsequently verified *via* RT−qPCR (Fig. 5abc). RT−qPCR (Fig. 5abc) revealed that EntLX expression in the gut epithelium and peritrophic membrane rapidly increased after feeding *E. faecalis* LX10 cells and reached a steady level after 4 and 6 days

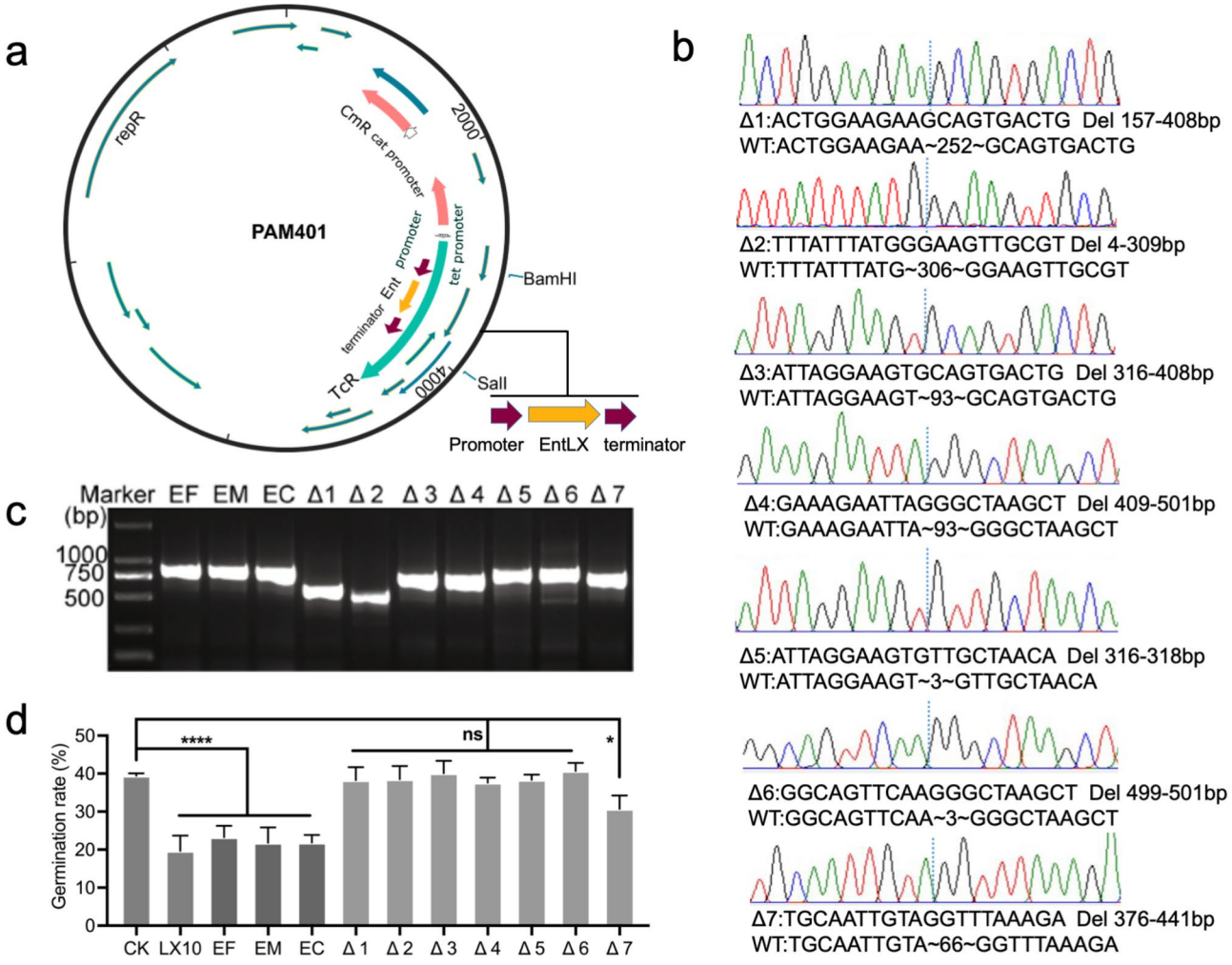

Fig. 3 Construction and activity measurement of engineered *Enterococcus* and insertional mutants. **(a)** Maps and cloning sites of the engineered *Enterococcus* construction system. The Enterococcus shuttle vector PAM401 drove the expression of both the promoter and the EntLX protein. Confirmation of engineered *Enterococcus* strains (EF, EM, EC) and insertion mutants (Δ1-Δ7) by PCR **(b)** and agarose gel electrophoresis **(c)**. Engineered strains harboring the EntLX genes of EF, EM, and EC inhibited *N. bombycis* germination compared with the germination of the *Enterococcus* strains without the EntLX gene (CK). **(d)** Validation of the anti-microspore activity of engineered *Enterococcus* strains (EF, EM, EC) and insertion mutants (Δ1-Δ7) in vitro. The results showed that disulfide bonding was essential for anti-*N. bombycis* activity

of treatment (Fig. 5ab). For example, the expression level of EntLX in the peritrophic membrane reached 8-fold greater on Day 6 than that in the CK group (Fig. 5b). The expression levels of EntLX tended to increase first and then decrease (Fig. 4c). However, we detected EntLX expression in the gut tissue but not in the hemolymph, suggesting that *E. fecalis* LX10-secreted EntLX cannot penetrate other tissues through the gut.

Histological sections showing general and detailed views of the silkworm gut (Fig. 5d-g). Both the CK- and EntLX-treated groups exhibited clear microvilli on the surface of the epithelial cells and intact gut morphology (Fig. 5de). The silkworms treated with *N. bombycis* displayed classic signs of infection, including spore invasion of the epithelium, vacuolation of intracellular organelles, and distension of the distal ends of the goblet cells (Fig. 5f). In contrast, silkworms treated with EntLX (2 mg/mL) exhibited significantly reduced invasion of *N. bombycis in vivo*, with epithelial cells surrounding basement membranes remaining intact. Although the microvilli were destroyed, there were no signs of damage to other intestinal tissues at this stage (Fig. 5g).

E. faecalis LX10 regulates metabolic homeostasis in silkworm

Metabolic status impacts the physiological function and economic traits of the host, we further examined the association of *N. bombycis* and *E. faecalis* LX10 *larvae* by applying an untargeted metabolomics. In total, 526 and 414 metabolites were detected by the positive (POS) and negative (NEG) models, respectively, 389 and 302 of which were annotated. We obtained a total of 215 KEGG

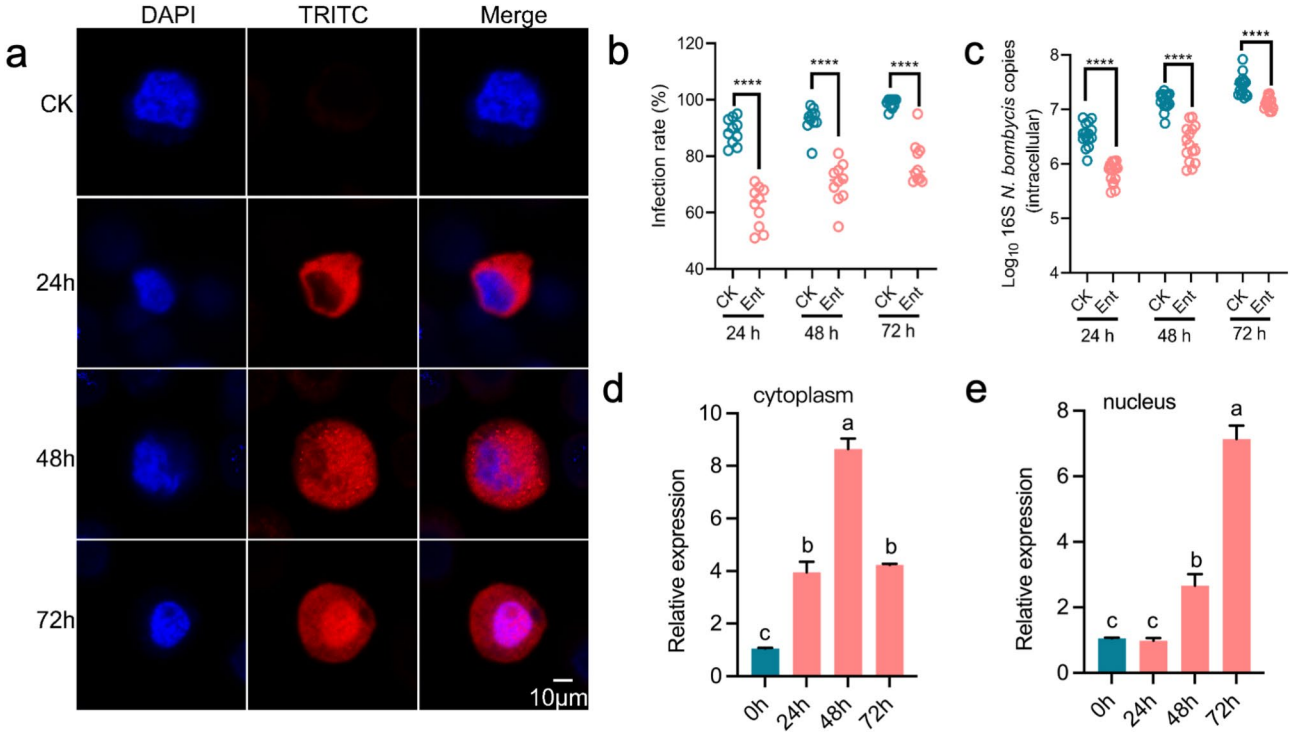

Fig. 4 Subcellular localization of the BmN transgenic cell line and the expression level of EntLX determined *via* qPCR. **(a)** Subcellular localization of EntLX as demonstrated by immunofluorescence *via* confocal microscopy.cell nucleus (DAPI; blue), anti-EntLX antibody (EntLX; red), and merged images. **(b)** BmN cells were infected with *N. bombycis* at 10^7 spores/mL, and the cell infection rate was determined *via* light microscopy. The percentage of *N. bombycis* infection was calculated for the CK group and transfected cell groups. **(c)** DNA was extracted from the control and transfected cell groups, and *N. bombycis* intracellular burden was estimated *via* qPCR. The infection rate and number of spore copies of *N. bombycis* were significantly reduced. Four asterisks (****) represent significant differences ($P < 0.0001$). **(d, e)** RT–PCR analysis of the specific expression of EntLX by Ent F/R in BmN transgenic cells. All assays were carried out in triplicate

orthologs, which were detected and classified into 15 categories according to gene pathway at level 2 against the KEGG database. Several nutrients were found in the intestinal epithelial, including amino acids (34.4%), carbohydrates (23.8%), lipids (18.6%) and nucleotides (11.6%) (Fig. 6A).

The PLS-DA analysis showed obvious differences among the CK, EF (*E. faecalis* LX10), NB (*N. bombycis*), and NF (*E. faecalis* LX10 + *N. bombycis*) samples without overfitting, especially on different days (Fig. 6b, Supplementary Fig. 2). There were 133 metabolites that showed significant differences between *E. faecalis* LX10 larvae and normal larvae (CK), and 179 metabolites that showed significant differences between *N. bombycis* larvae and CK group. Interestingly, after simultaneous feeding with *E. faecalis* LX10 and *N. bombycis* (NF) for 6 d, the metabolites showed different degrees of recovery and correction (Fig. 6c). The differentially abundant metabolites between the different groups at 2 d and 4 d exhibited similar trends (Fig. 6c). From a pathway topology analysis perspective, alanine, aspartate and glutamate metabolism; arginine biosynthesis; purine metabolism; starch and sucrose metabolism; pyrimidine metabolism; and glycerophospholipid metabolism were the pathways with the highest impact after *N. bombycis* treatment (Fig. 6d). The six perturbed metabolic pathways exhibited greater pathway impact values and lower *P* values after infected with *N. bombycis*. In addition, the pathway impact and *P* value were somewhat correlated with those of healthy silkworms, suggesting that these changes may be important features regulating host resistance against *N. bombycis* (Fig. 6d).

E. faecalis LX10 regulates the physiological function and economic traits of silkworms

To verify that *E. faecalis* LX10 plays a role in host resistance against *N. bombycis*, the larval mass and economic traits of the silkworms were investigated. There was a significant ($P < 0.05$) decrease in larval mass after treatment with *N. bombycis* after infection (2 d, 4 d and 6 d) (Fig. 7a-c). The economic traits (cocoon length, cocoon width, whole-cocoon weight, cocoon shell weight, pupation rate and adult emergence rate) exhibited similar trends (Fig. 7d-i). The *E. faecalis* LX10-fed group did not differ significantly from the CK group in terms of larval mass or economic trait parameters, suggesting that 10^7 CFU/mL of bacteria was not toxic ($P > 0.05$). Interestingly, a significant improvement in larval mass and

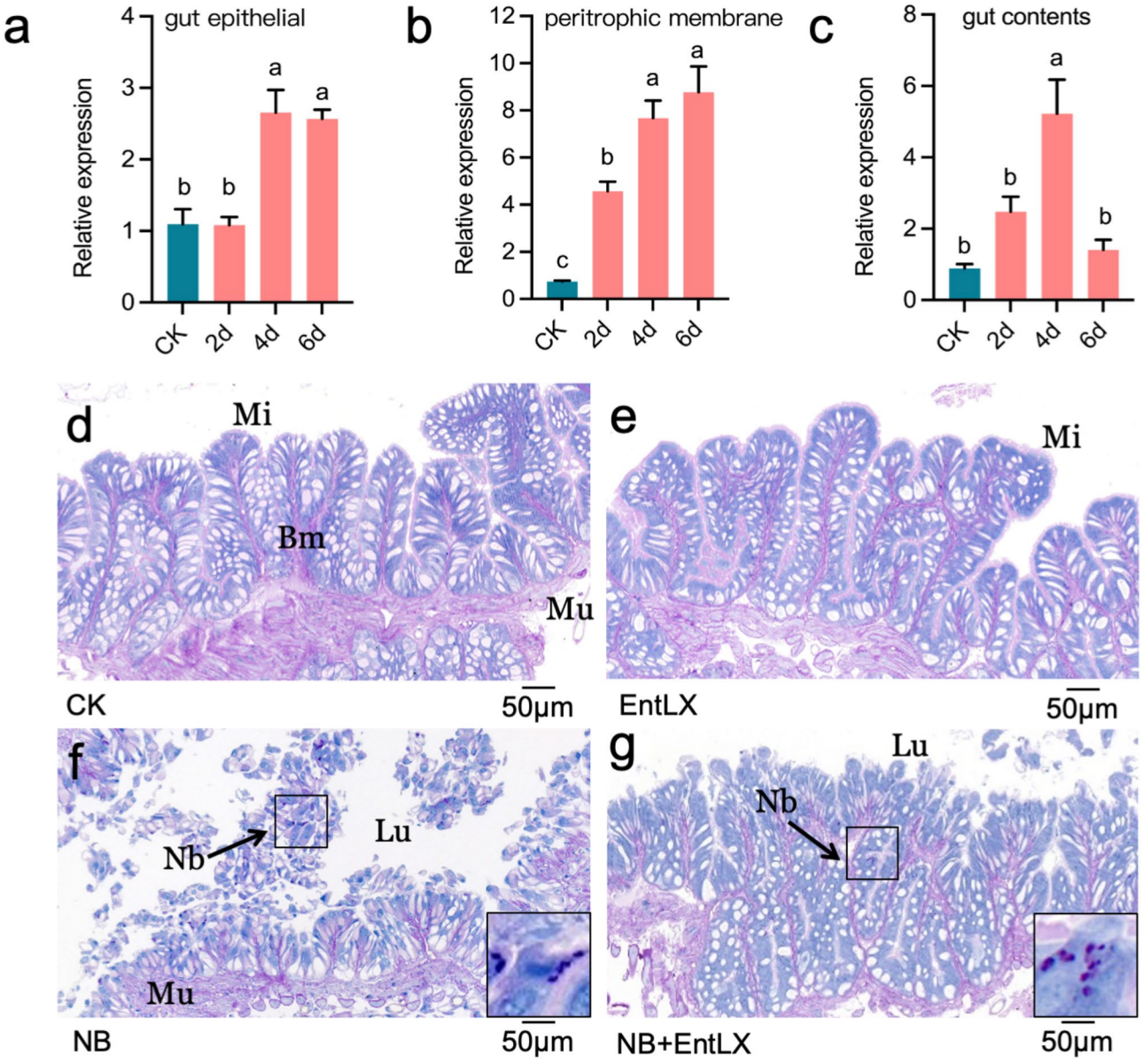

Fig. 5 Gut tissue-specific expression profiles of EntLX and its anti-*N. bombycis* effect in vivo. Tissue-specific expression of EntLX in silkworms was assessed using RT–qPCR **(a-c)**. **(a)** Gut epithelial; **(b)** peritrophic membrane; **(c)** gut contents. The guts of silkworms were excised for histological examination (PAS staining) after treatment with EntLX136 (**e**, EntLX, 2 mg/mL), *N. bombycis* (**f**, NB, 10^9 spores/mL), or *N. bombycis* and EntLX136 (**g**, EntLX + NB). The same volume of sterile water (CK, **d**) was provided as a control. Nb,*N. bombycis* spores; Bm, basement membrane; Lu, lumen; Mi, microvilli

economic trait parameters was observed after feeding *E. faecalis* LX10 as compared with *N. bombycis* inoculation alone. These findings were consistent with the metabolomics results.

To summarize, this investigation presents a comprehensive overview of the intricate interaction among *N. bombycis*, *B. mori*, and *E. faecalis* LX10. The robust anti-*N. bombycis* effect of EntLX secreted by *E. faecalis* LX10 was observed *via* four plausible mechanisms (Fig. 8): (i) reduce the infection efficiency of *N. bombycis* by biological modification, (ii) improve gut barrier function, (iii) regulate the metabolic homeostasis of the host and (iii) regulate the physiological function and economic traits of *B. mori.* Furthermore, we anticipate future applications such as the expression of therapeutic antimicrobial proteins through engineered probiotic bacteria controlled by intestinal commensal bacteria or even by pathogenic microorganisms.

Discussion

This work showed that EntLX is present in *E. faecalis* LX10 strains and encodes a 171 aa peptide according to complete genome sequencing. The enzyme gelatinase (GelE) secreted by *E. faecalis* LX10 cleaves EntLX into

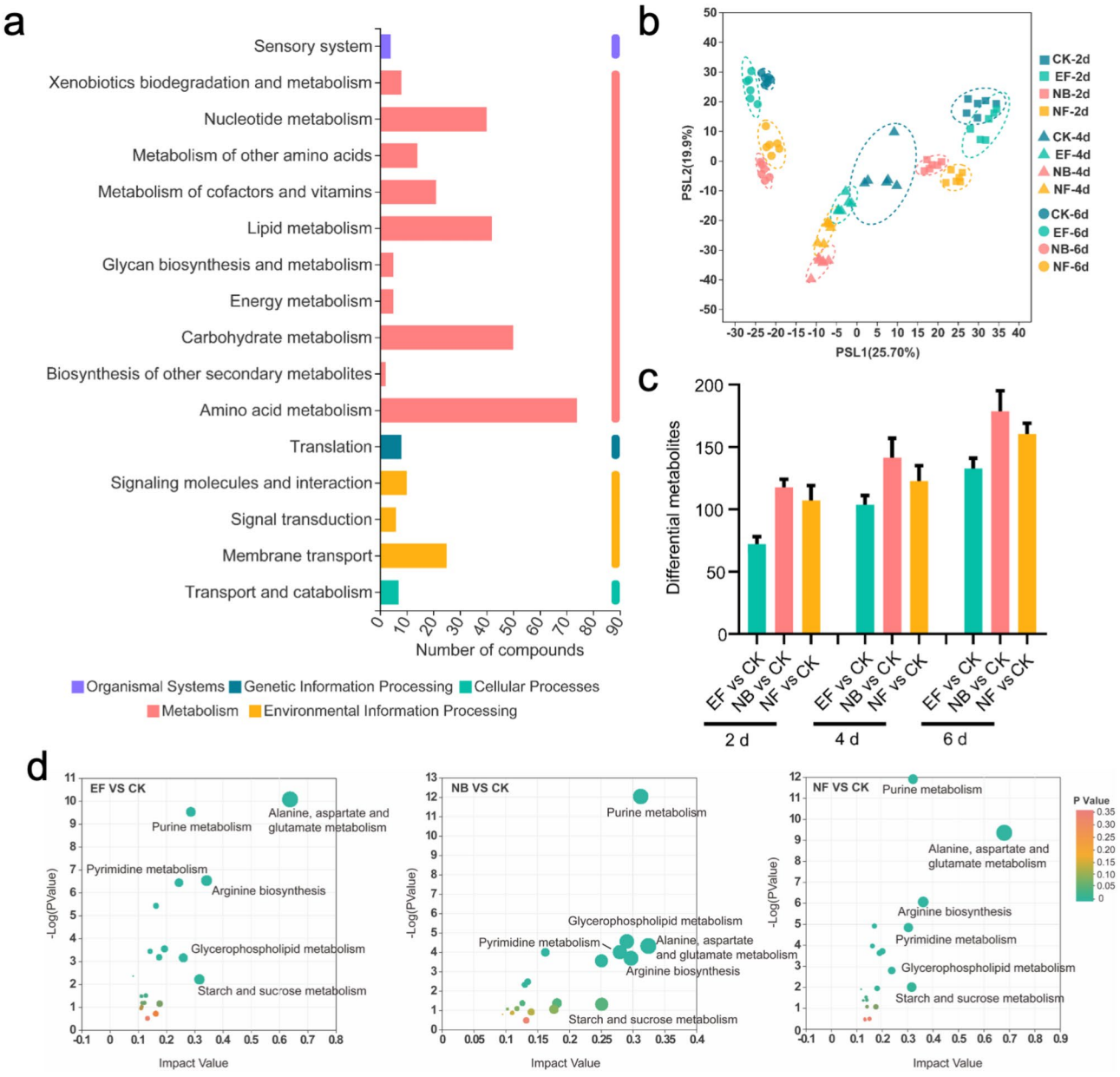

Fig. 6 The gut metabolome of silkworms and larvae associated with *E. faecalis* LX10 and *N. bombycis*. **(a)** KEGG pathway enrichment of the gut metabolites. **(b)** PLS-DA analysis of untargeted metabolomics data of healthy silkworm (CK), *E. faecalis* LX10 (EF, 10^7 CFU/mL), *N. bombycis* (NB, 10^9 spores/mL), and *E. faecalis* LX10 + *N. bombycis* (NF) group silkworms. Different processing times and groupings are visualized with different shapes and colours. **(c)** Pathway analysis of the identified differentially abundant metabolites in the CK, EF, NB, and NF groups. **(d)** Pathway impact resulting from the differentially abundant metabolites using MetaboAnalyst. The node color is based on the *P* values, and the node radius represents the pathway impact values

its active 68-amino-acid form and contributes to anti-*N. bombycis* activity. Other studies have shown that the Fsr system in *E. faecalis* regulates the activity of GelE protein, which modulates a range of physiological functions of organism [39]. GelEs are expressed in several bacteria, including *Enterococcus*, *Serratia marcescens* and *Pseudomonas aeruginosa*, and are members of the M4 family of proteases [40, 41]. An extensive range of substrates can be cleaved by GelEs, including gelatins; enterococcal proteins; and factors, such as hemoglobin, endothelin, laminin and collagen, all of which play integral roles in the physiology of *E. faecalis* [42–45]. For example, Fsr mediates Ace surface levels through its regulation of the metalloprotease gelatinase (GelE), which we showed directly cleaves Ace, subsequently impacting the ability of cells to adhere to collagen [35]. Cleavage of enterococcin by gelatinase plays a crucial role in its bacteriocin activity and the modulation of *Candida albicans* hyphal formation [34]. Therefore, we hypothesize that the signal peptide is cleaved during secretion releasing a 136 amino

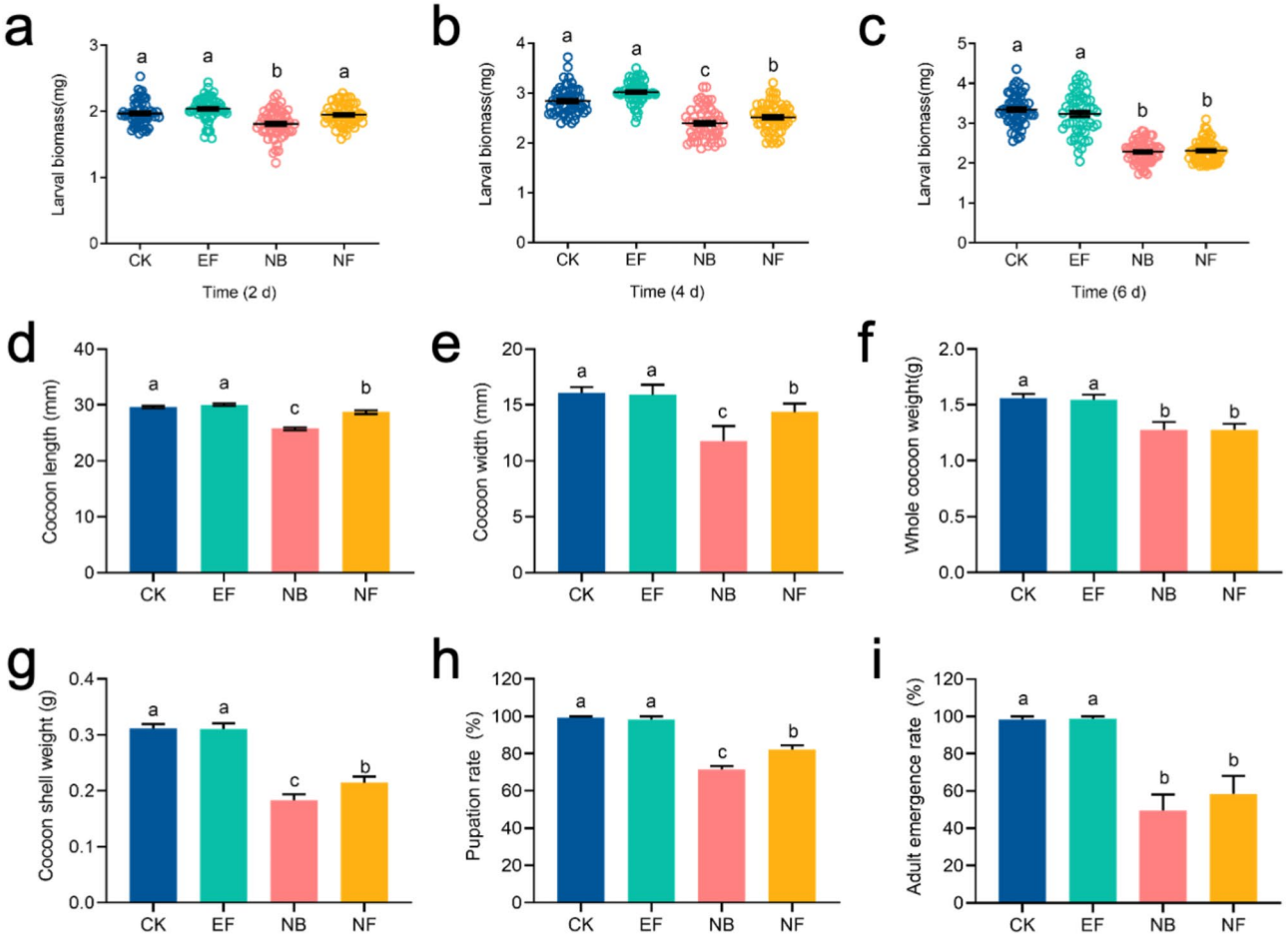

Fig. 7 Effect of *E. faecalis* LX10 on physiological function and economic traits after silkworm infection with *N. bombycis*. Larval masses of the different groups (mean with 95% confidence interval, $n = 60$ for each group) after 2 d **(a)**, 4 d **(b)** and 6 d **(c)**. **(d)** Cocoon length, **(e)** cocoon width, **(f)** whole-cocoon weight, **(g)** cocoon shell weight, **(h)** pupation rate and **(i)** adult emergence rate of the healthy silkworm (CK), *E. faecalis* LX10 (EF, 10^7 CFU/mL), *N. bombycis* (NB, 10^9 spore/mL), and *E. faecalis* LX10 + *N. bombycis* (NF) group silkworms

acid protein. The protein is further cleaved in half by the extracellular protease GelE, generating the active form of EntLX which comprises the 68 amino acid C-terminus.

We also showed that the anti-*N. bombycis* activity of EntLX is dependent on disulfide bonds and DsbA. Additionally, an N-terminal signal peptide (103 aa) in nascent EntLX interacts with DsbA, which is predicted to be directly secreted, as previously demonstrated in other bacteria [34, 46–48]. Many secreted proteins rely on disulfide bonds to maintain their stability and function in gram-positive or gram-negative bacteria [46, 48]. The antimicrobial protein SA-M57, the enterococcal V583, and the corynicin JK, derived from *Streptococcus pyogenes*, *E. faecalis*, and *Corynebacterium jeikeium*, contain an essential disulfide bond [47]. When proteins, like EntLX, are secreted, the DsbA protein is placed in a favorable position to facilitate the formation of disulfide bonds [48]. The thiol-disulfide oxidoreductases are closely associated with specific bacteriocins. The lantibiotic sublancin 168, a disulfide-bonded bacteriocin encoded by the same operon as the oxidoreductases bdbA and bdbB, is encoded by *Bacillus subtilis* [49]. *E. faecalis* F4-9 contains a gene encoding a bacteriocin called enterocin F4-9 adjacent to a gene needed to form thiol-disulfide oxidoreductases [50, 51]. Related studies have found that that *E. faecalis* produces a small protein that is a potent inhibitor of the ability of *C. albicans* to form biofilms and reduces fungal virulence. Additionally, a disulfide bond, which essentially joins the N and C termini of the cleaved form of small protein, was shown to form and be necessary for bacteriocin activity [37]. This aligns with previous findings showing that A predicted disulfide bond encompasses nearly the entire length of the active peptide (amino acids 4–65) and is necessary for its antibacterial activity [34].

In addition, we used engineered strains and transgenic cells that express EntLX to prevent *N. bombycis* infection *via* ligand–receptor interactions. We have shown that the EF, EM and EC strains but not the parental WT strain dramatically reduced the germination rate of *N.*

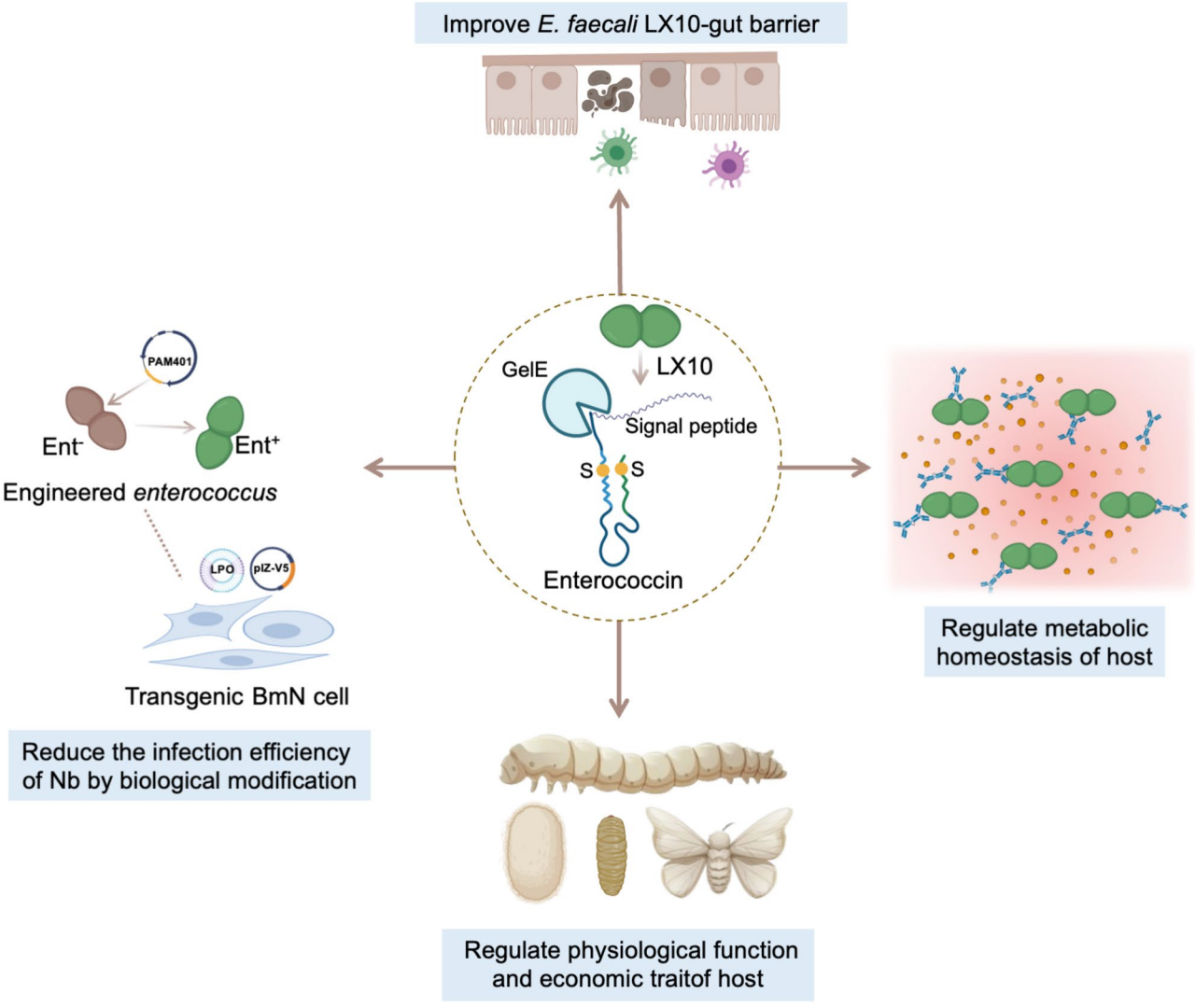

Fig. 8 Schematics showing the mechanism of *E. faecalis* LX10 against *N. bombycis*. *E. faecalis* prevents *N. bombycis* infection by four plausible mechanisms: (i) reduce the infection efficiency of *N. bombycis* by biological modification, (ii) improve gut barrier function, (iii) regulate metabolic homeostasis of the host and (iii) regulate the physiological function and economic traits of *B. mori*

bombycis. The approach of engineering probiotics and transgenic cells with EntLX from a nonpathogenic bacterium to exclude pathogens significantly enhances prophylactic use without causing serious health problems and thus provides effective prevention of *N. bombycis* infection. Applying probiotic bacteria as a strategy to counteract intestinal pathogens is a rational approach. Research conducted in the past has demonstrated that an adhesion protein synthesized by *Lactobacillus salivarious* of engineered probiotics could control *Listeria* infection in mice by increasing intestinal immunomodulatory functions or competing with intestinal receptor binding to the toxins [52]. Furthermore, the engineered strains *Enterobacter* sp. E5P and *Kosakonia* sp. S1P significantly increase *Fusarium* resistance by expressing 1-aminocyclopropane-1-carboxylate (ACC) deaminase [53]. As far as transgenic cells are concerned, there are many precedents for success. For example, BmAtlastin transgenic cell line of silkworm BmN cells could enhance resistance to BmNPV [54].

The EntLX protein secreted by *E. faecalis* LX10 is abundantly expressed in intestinal tissues, including the gut epithelium, peritrophic membrane and contents. Previous studies have reported that bacteriocin secreted by gut-inhabiting bacteria is an important determinant of gut homeostasis and host-microbiome interactions [55, 56]. In the present study, EntLX was detected only in gut tissue and could not penetrate other tissues through the gut. This is probably because *E. faecalis* can proliferate within a certain threshold range in the silkworm gut only in the *B. mori-E. faecalis* colonization model. A feeding dose of 10^7 CFU/silkworm was found to be the

most effective for colonization [57]. Probiotics may represent "exogenous" microflora that exert a local beneficial effect, and successfully colonized microflora permanently exert such an effect during intestinal organization [58]. In addition, the subcelluar localization of EntLX might be part of the BmN cell's response to *N. bombycis* infection. Similarly, the infection of BmN cells by *N. bombycis* is a multi-step process that begins with spore attachment and germination, followed by the injection of sporoplasm into the cytoplasm and eventually reach the nucleus. During infection or stress, EntLX often migrate from the cytoplasm to the nucleus, where they initiate defensive gene expression programs against *N. bombycis* infection (unpublished). Many physiological features of the intestinal microecological environment, including strongly alkaline digestive juices, nutrient availability, and antimicrobial agents, inhibit the immortal proliferation of gut microbes [59]. Using a *B. mori* model of *N. bombycis* infection, we discovered that EntLX reduced but not eliminated *N. bombycis* infection. Similarly, the existence of *E. faecalis* hindered the morphogenesis of *C. albicans* but not completely; this inhibition prevented tissue damage caused by hyphal expansion in *Caenorhabditis elegans* infection models [39, 60]. It is possible that *N. bombycis* and *E. faecalis* cooperate to promote colonization; this interaction would allow nonpathogenic bacteria to remain associated in the host for long periods of time.

After simultaneous feeding with *E. faecalis* LX10 and *N. bombycis*, the differentially abundant metabolites showed different degrees of correction and recovery compared with simple infections with *N. bombycis*, including amino acid metabolites, purine metabolism and starch and sucrose metabolism. For example, monoassociation of germ-free silkworms with *Stenotrophomonas* to produce high levels of amino acids enhances host biological fitness and survival under insecticide stress [30]. In addition, insects provide the energy required for growth and development through starch and sucrose metabolism, and store energy in the form of glycogen [61]. The beneficial effects of commensal bacteria could be exerted through barrier functions of the gut or by providing essential nutritional supplements for host metabolic homeostasis, suggesting that probiotics may play a role in inducing anti-inflammatory signals [62]. Ménard et al. reported that *Streptococcus thermophilus* and *Bifidobacterium breve* release metabolites that exert an antitumor necrosis factor alpha (TNF-α)-mediated effect capable of filtering grown intestinal epithelial cell monolayers [58]. We hypothesize that *E. faecalis* LX10, through colonization of the silkworm gut, indirectly enhances the silkworm's resistance to infection by stimulating the secretion of key metabolites, thereby improving its overall biological fitness. In our study, after treatment with 10^7 CFU/mL *E. faecalis* LX10, the larval mass and economic parameters were significantly greater than those observed in response to *N. bombycis* infection alone; these parameters are positively correlated with health conditions and induced better growth of silkworms. These traits are key factors in improving the quality of silkworm breeds, maintaining trait stability, promoting growth and development, and optimizing sericulture. Improving these economic traits not only promotes technological advancements in the silk industry but also drives its sustainable development, enhancing its competitiveness in the global market [63]. From an ecological perspective, these traits reflect the adaptability of silkworm populations to environmental factors. Overall, these economic traits and ecological factors play a critical role in enhancing the sustainable development of the silk industry [64]. Furthermore, it is plausible that the interaction between *E. faecalis* LX10 and *N. bombycis* leads to the initiation of an enzymatic process, resulting in the synthesis of EntLX that effectively hinders the germination of EntLX. Additionally, increasing the nutritional level of a host confers a significant fitness advantage, which increases host tolerance to *N. bombycis*. Our findings demonstrate that the natural symbiotic bacterium *E. faecalis* LX10 drives *B. mori* refractoriness to *N. bombycis* infection *via* the secretion of EntLX.

To summarize, this investigation presents a comprehensive overview of the intricate interaction among *N. bombycis*, *B. mori*, and *E. faecalis* LX10. The robust anti-*N. bombycis* effect of EntLX secreted by *E. faecalis* LX10 was observed *via* four plausible mechanisms (Fig. 8): (i) reduce the infection efficiency of *N. bombycis* by biological modification, (ii) improve gut barrier function, (iii) regulate the metabolic homeostasis of the host and (iv) regulate the physiological function and economic traits of *B. mori.* The potential of peptides to broaden the pool of antimicrobial agents has been increasingly recognized. These discoveries demonstrate that the enhancement of antifungal activity from naturally occurring peptides is possible. Furthermore, we anticipate future applications such as the expression of therapeutic antimicrobial proteins through engineered probiotic bacteria controlled by intestinal commensal bacteria or even by pathogenic microorganisms. In this regard, peptides derived from EntLX are promising leads for further optimization and development. However, *E. faecalis* LX10 represents only a single species among the myriad microorganisms inhabiting the silkworm gut. Further studies on the safety and stability of *E. faecalis* LX10 bacteria or purified EntLX in the gut environment, as well as their competition with native microbiota, are needed to investigate the potential role of these bioactive

molecules in controlling *N. bombycis* infection in silkworms.

Abbreviations

BmN cells	Ovarian cell line of *Bombyx mori*
EntLX	The enterococcal protein
RT-qPCR	Real-time quantitative PCR

Supplementary Information

The online version contains supplementary material available at https://doi.org/10.1186/s12866-025-03980-y.

Supplementary Material 1

Supplementary Material 2

Acknowledgements
We thank AJE (https://www.aje.cn) for its linguistic assistance during the preparation of this manuscript.

Author contributions
XZ and LY performed the experiments and analyzed the data. TC, HL and XZ drafted the manu-script and performed manuscript preparation. PC, NG, YG and ZY supervised and performed the collection of material. XZ, XL, FZ and CW conceived the idea and coordinated the project. All authors have read and agreed to the published version of the manuscript.

Funding
This research was funded by the China Agriculture Research System of MOF and MARA, Scientific Research Fund of Zhejiang Provincial Education Department (Y20235377), Zhejiang Provincial Natural Science Foundation of China under Grant No. LQN25C170001, and Huzhou Science and Technology Bureau (2024YZ07).

Data availability
The whole genome sequencing generated and analysed during the current study are available in the NCBI BioProjects repository: PRJNA810349 and CP092784-CP092785. The untargeted metabolomics analysis data were deposited into the MetaboLights database under accession number MTBLS9220, www.ebi.ac.uk/metabolights/MTBLS9220.

Declarations

Ethics approval and consent to participate
Not applicable.

Consent for publication
Not applicable.

Competing interests
The authors declare no competing interests.

Author details
[1]School of Life Science, Huzhou University, Huzhou 313000, China
[2]Laboratory of Invertebrate Pathology, College of Animal Sciences, Zhejiang University, Hangzhou 310058, China
[3]Institute of Sericulture, Huzhou Academy of Agricultural Sciences, Huzhou 313002, China
[4]College of Life Science, Shandong Normal University, Jinan 250358, China
[5]Shandong Center for Disease Control and Prevention, Jinan 250014, China

Received: 10 December 2024 / Accepted: 21 April 2025
Published online: 17 May 2025

References

1. Solter LF. Epizootiology of microsporidiosis in invertebrate hosts. 2014.
2. Didier ES. Microsporidiosis: an emerging and opportunistic infection in humans and animals. Acta Trop. 2005;94:61–76.
3. Han B, Weiss LM. Microsporidia: obligate intracellular pathogens within the fungal Kingdom. Microbiol Spectr. 2017;5.
4. Becnel JJ, Andreadis T. Microsporidia in insect. In: Wittner M, Weiss LM, editors. The microsporidia and microsporidiosis. Washington DC: ASM; 1999. pp. 447–501.
5. Fang W, Zhou L, Deng B, Guo B, Chen X, Chen P, et al. Establishment of a secretory Protein-Inducible CRISPR/Cas9 system for Nosema Bombycis in insect cells. J Agric Food Chem. 2024;72:13175–85.
6. Singh T, Bhat MM, Khan MA. Microsporidiosis in the silkworm, *Bombyx mori* L. (Lepidoptera: Bombycidae). Pertanika J Trop Agric Sci. 2012;35:387–406.
7. Bicart-Sée AMP, Linas MD, Datry A. Successful treatment with Nitazoxanide of *Enterocytozoon bieneusi* microsporidiosis in a patient with AIDS. Antimicrob Agents Chemother. 2000;44.
8. Dong Z, Zheng N, Hu C, Huang X, Chen P, Wu Q, et al. Genetic bioengineering of overexpressed guanylate binding protein family BmAtlastin-n enhances silkworm resistance to *Nosema bombycis*. Int J Biol Macromol. 2021;172:223–30.
9. Suraporn S, Terenius O. Supplementation of Lactobacillus casei reduces the mortality of *Bombyx mori* larvae challenged by *Nosema Bombycis*. BMC Res Notes. 2021;14:398.
10. Zheng S, Huang Y, Huang H, Yu B, Zhou N, Wei J, et al. The role of NbTMP1, a surface protein of sporoplasm, in *Nosema Bombycis* infection. Parasit Vectors. 2021;14:81.
11. Miao ZB, Zhang PF, Zhang Y, Huang XH, Liu JX, Wang GW. Single-cell analysis reveals the effects of glutaraldehyde and formaldehyde on individual *Nosema Bombycis* spores. Analyst. 2019;144:3136–43.
12. Wang Z, Liao F, Lin J, Li W, Zhong Y, Tan P, et al. Inactivation and mechanisms of Chlorine dioxide on *Nosema bombycis*. J Invertebr Pathol. 2010;104:134–9.
13. Liao S, Yang Q, Xing D, Xiao Y, Ye M, Li Q. A brief introduction to the whole control and prevention technology system against *Bombyx mori* pebrine disease. Acta Sericologica Sinica. 2016;42:148–51.
14. Boohene CK, Geden CJ, Becnel JJ. Evaluation of remediation methods for *Nosema* disease in *Muscidifurax raptor* (Hymenoptera: Pteromalidae). Environ Entomol. 2003;32:1146–53.
15. Costa SF, Weiss LM. Drug treatment of microsporidiosis. Drug Resist Updat. 2000;3:384–99.
16. Barretto DA, Gadwala M, Vootla SK. The silkworm gut microbiota: A potential source for biotechnological applications. Methods Silkworm Microbiol. 2021;49:1–26.
17. Zhu Q, Li F, Shu Q, Feng P, Wang Y, Dai M, et al. Disruption of peritrophic matrix Chitin metabolism and gut immune by Chlorantraniliprole results in pathogenic bacterial infection in *Bombyx mori*. Pestic Biochem Physiol. 2023;193:105430.
18. Shu Q, Guo X, Tian C, Wang Y, Zhang X, Cheng J et al. Homeostatic regulation of the Duox-ROS defense system: revelations based on the diversity of gut Bacteria in silkworms (*Bombyx mori*). Int J Mol Sci. 2023;24.
19. Li B, Zhang B, Zhang F, Liu X, Zhang Y, Peng W, et al. Interaction between dietary lactoferrin and gut microbiota in host health. J Agric Food Chem. 2024;72:7596–606.
20. Karczewski J, Troost FJ, Konings I, Dekker J, Kleerebezem M, Brummer RJ, et al. Regulation of human epithelial tight junction proteins by *Lactobacillus plantarum* in vivo and protective effects on the epithelial barrier. Am J Physiol Gastrointest Liver Physiol. 2010;298:G851–9.
21. Bron PA, Kleerebezem M, Brummer RJ, Cani PD, Mercenier A, MacDonald TT, et al. Can probiotics modulate human disease by impacting intestinal barrier function? Br J Nutr. 2017;117:93–107.
22. Suez J, Zmora N, Segal E, Elinav E. The pros, cons, and many unknowns of probiotics. Nat Med. 2019;25:716–29.
23. Kamada N, Chen GY, Inohara N, Nunez G. Control of pathogens and pathobionts by the gut microbiota. Nat Immunol. 2013;14:685–90.
24. Amalaradjou MA, Bhunia AK. Modern approaches in probiotics research to control foodborne pathogens. Adv Food Nutr Res. 2012;67:185–239.
25. Pagnini C, Saeed R, Bamias G, Arseneau KO, Pizarro TT, Cominelli F. Probiotics promote gut health through stimulation of epithelial innate immunity. Proc Natl Acad Sci U S A. 2010;107:454–9.
26. Klaenhammer TR, Kleerebezem M, Kopp MV, Rescigno M. The impact of probiotics and prebiotics on the immune system. Nat Rev Immunol. 2012;12:728–34.

27. Somers E, Amke A, Croonenborghs A, van Overbeek LS, Vanderleyden J. Lactic acid bacteria in organic agricultural soils. Poster session presented at Rhizosphere 2; Montpellier, France. p. 26–31.
28. Kumar D, Sun Z, Cao G, Xue R, Hu X. Gong CJJoA-PE. Study of gut bacterial diversity of *Bombyx mandarina* and *Bombyx mori* through 16S rRNA gene sequencing. J Asia-Pac Entomol. 2019;22:522–30.
29. Zhang X, Feng H, He J, Liang X, Zhang N, Shao Y, et al. The gut commensal bacterium *Enterococcus faecalis* LX10 contributes to defending against *Nosema Bombycis* infection in *Bombyx mori*. Pest Manag Sci. 2022;78:2215–27.
30. Chen B, Zhang N, Xie S, Zhang X, He J, Muhammad A, et al. Gut bacteria of the silkworm *Bombyx mori* facilitate host resistance against the toxic effects of organophosphate insecticides. Environ Int. 2020;143:105886.
31. Pospiech A, Neumann B. A versatile quick-prep of genomic DNA from gram-positive bacteria. Trends Genet. 1995;11:217-8.
32. Nguyen H, Tran D, Tran B, Roy M, Cassell A, Dascalu S, et al. SMRT: randomized data transformation for Cancer subtyping and big data analysis. Front Oncol. 2021;11:725133.
33. Hancock LE, Perego M. The *Enterococcus faecalis* Fsr two-component system controls biofilm development through production of gelatinase. J Bacteriol. 2004;186:5629–39.
34. Dundar H, Brede DA, La Rosa SL, El-Gendy AO, Diep DB, Nes IF. The Fsr Quorum-Sensing system and cognate gelatinase orchestrate the expression and processing of proprotein EF_1097 into the mature antimicrobial peptide enterocin O16. J Bacteriol. 2015;197:2112–21.
35. Pinkston KL, Gao P, Diaz-Garcia D, Sillanpaa J, Nallapareddy SR, Murray BE, et al. The Fsr quorum-sensing system of *Enterococcus faecalis* modulates surface display of the collagen-binding MSCRAMM Ace through regulation of GelE. J Bacteriol. 2011;193:4317–25.
36. Goujon JM, Hauet T, Menet E, Levillain P, Babin P, Carretier M. Histological evaluation of proximal tubule cell injury in isolated perfused pig kidneys exposed to cold ischemia. J Surg Res. 1999;82:228–33.
37. Graham CE, Cruz MR, Garsin DA, Lorenz MC. *Enterococcus faecalis* bacteriocin EntV inhibits hyphal morphogenesis, biofilm formation, and virulence of *Candida albicans*. Proc Natl Acad Sci U S A. 2017;114:4507–12.
38. Nocek BP, Li H, Collart F, JA MCSG. Structure of a conserved hypothetical protein from *Enterococcus faecalis* V583. PDB 1Z6M. 2005;Accession number: Q837R1.
39. Cruz MR, Graham CE, Gagliano BC, Lorenz MC, Garsin DA. *Enterococcus faecalis* inhibits hyphal morphogenesis and virulence of *Candida albicans*. Infect Immun. 2013;81:189–200.
40. Del Papa MF, Hancock LE, Thomas VC, Perego M. Full activation of *Enterococcus faecalis* gelatinase by a C-terminal proteolytic cleavage. J Bacteriol. 2007;189:8835–43.
41. Sam MR, Ghoreishi S. Prodigiosin produced by *Serratia marcescens* inhibits expression of MMP-9 and survivin and promotes caspase-3 activation with induction of apoptosis in acute lymphoblastic leukaemia cells. J Appl Microbiol. 2018;125:1017–29.
42. MacCallum WGHT. A case of acute endocarditis caused by Micrococcus zymogenes (nov. spec.), with a description of the microorganism. J Exp Med. 1899;4:521–34.
43. Thomas VC, Thurlow LR, Boyle D, Hancock LE. Regulation of autolysis-dependent extracellular DNA release by *Enterococcus faecalis* extracellular proteases influences biofilm development. J Bacteriol. 2008;190:5690–8.
44. Thurlow LR, Thomas VC, Narayanan S, Olson S, Fleming SD, Hancock LE. Gelatinase contributes to the pathogenesis of endocarditis caused by *Enterococcus faecalis*. Infect Immun. 2010;78:4936–43.
45. Brown AO, Graham CE, Cruz MR, Singh KV, Murray BE, Lorenz MC et al. Antifungal activity of the *Enterococcus faecalis* peptide EntV requires protease cleavage and disulfide bond formation. mBio. 2019;10:e01334-19..
46. Dumoulin A, Grauschopf U, Bischoff M, Thony-Meyer L, Berger-Bachi B. *Staphylococcus aureus* DsbA is a membrane-bound lipoprotein with thiol-disulfide oxidoreductase activity. Arch Microbiol. 2005;184:117–28.
47. Swe PM, Heng NCK, Ting YT, Baird HJ, Carne A, Tauch A, et al. ef1097 and YpkK encode enterococcin V583 and Corynicin JK, members of a new family of antimicrobial proteins (bacteriocins) with modular structure from Gram-positive bacteria. Microbiol (Reading). 2007;153:3218–27.
48. Reardon-Robinson ME, Ton-That H. Disulfide-Bond-Forming pathways in Gram-Positive Bacteria. J Bacteriol. 2015;198:746–54.
49. Dorenbos R, Stein T, Kabel J, Bruand C, Bolhuis A, Bron S, et al. Thiol-disulfide oxidoreductases are essential for the production of the lantibiotic Sublancin 168. J Biol Chem. 2002;277:16682–8.
50. Maky MA, Ishibashi N, Zendo T, Perez RH, Doud JR, Karmi M, et al. Enterocin F4-9, a novel O-Linked glycosylated bacteriocin. Appl Environ Microbiol. 2015;81:4819–26.
51. Maky MA, Ishibashi N, Nakayama J, Zendo T. Characterization of the biosynthetic gene cluster of enterocin F4-9, a glycosylated bacteriocin. Microorganisms. 2021;9:2276.
52. Drolia R, Amalaradjou MAR, Ryan V, Tenguria S, Liu D, Bai X, et al. Receptor-targeted engineered probiotics mitigate lethal *Listeria* infection. Nat Commun. 2020;11:6344.
53. Liu Y, Zhu A, Tan H, Cao L, Zhang R. Engineering banana endosphere Microbiome to improve *Fusarium wilt* resistance in banana. Microbiome. 2019;7:74.
54. Liu TH, Dong XL, Pan CX, Du GY, Wu YF, Yang JG, et al. A newly discovered member of the Atlastin family, BmAtlastin-n, has an antiviral effect against BmNPVin *Bombyx mori.* Sci Rep. 2016;6:28946.
55. Ormerod KL, Wood DL, Lachner N, Gellatly SL, Daly JN, Parsons JD, et al. Genomic characterization of the uncultured Bacteroidales family S24-7 inhabiting the guts of homeothermic animals. Microbiome. 2016;4:36.
56. Chagwedera DN, Ang QY, Bisanz JE, Leong YA, Ganeshan K, Cai J, et al. Nutrient sensing in CD11c cells alters the gut microbiota to regulate food intake and body mass. Cell Metab. 2019;30:364–73. e7.
57. Zhang X, Feng H, He J, Muhammad A, Zhang F, Lu X. Features and colonization strategies of *Enterococcus faecalis* in the gut of *Bombyx mori*. Front Microbiol. 2022;13:921330.
58. Menard S, Candalh C, Bambou JC, Terpend K, Cerf-Bensussan N, Heyman M. Lactic acid bacteria secrete metabolites retaining anti-inflammatory properties after intestinal transport. Gut. 2004;53:821–8.
59. Zhang X, Zhang F, Lu X. Diversity and functional roles of the gut microbiota in lepidopteran insects. Microorganisms. 2022;10:1234.
60. Garsin DA, Lorenz MC. Candida albicans and *Enterococcus faecalis* in the Gut: synergy in commensalism? Gut Microbes. 2013;4:409–15.
61. Reyes-DelaTorre A, Teresa M, Rafael J. Carbohydrate metabolism in drosophila: reliance on the disaccharide Trehalose. Carbohydrates - Comprehensive Studies on Glycobiology and Glycotechnology; 2012.
62. Neish AS, Gewirtz AT, Zeng H, Young AN, Hobert ME, Karmali V, et al. Prokaryotic regulation of epithelial responses by Inhibition of IkappaB-alpha ubiquitination. Science. 2000;289:1560–3.
63. Neshagaran Hemmatabadi R, Seidavi A, Gharahveysi S. A review on correlation, heritability and selection in silkworm breeding. J Appl Anim Res. 2014;44:9–23.
64. Kumar UA, Parasuramudu M, Nandhini K, Reddy YP. Optimizing silkworm rearing: the impact of environmental factors and advanced technologies on silk quality and production. Res Biotica. 2024;3:195–202.

Publisher's note